

Electronic structure of single-layered undoped cuprates from hybrid density functional theory

Pablo Rivero, Ibério de P.R. Moreira, and Francesc Illas

Departament de Química Física and Institut de Química Teòrica i Computacional (IQTCUB), Universitat de Barcelona, C/Martí i Franquès 1, E-08028 Barcelona, Spain

(Received 18 February 2010; revised manuscript received 30 April 2010; published 28 May 2010)

The ability of different periodic density functional theory-based methods to correctly describe the electronic structure and magnetic properties of La_2CuO_4 , $\text{Ca}_2\text{CuO}_2\text{Cl}_2$, $\text{Sr}_2\text{CuO}_2\text{F}_2$, and $\text{Sr}_2\text{CuO}_2\text{Cl}_2$ as representative of simple monolayered high- T_c superconducting cuprate parent compounds is explored. Plane waves (PW) and atomic Gaussian-type orbitals (GTO) have been used to represent the electron density of the systems. It is shown that (i) for a given exchange-correlation potential, both PW and GTO basis sets provide an equivalent description; (ii) standard local density approximation (LDA) and generalized gradient approximation (GGA) methods predict an incorrect metallic ground state with a very poor spin density at Cu sites which is in contradiction to experimental evidence showing that these systems behave as charge transfer antiferromagnetic insulators with spin density localized mainly at the Cu sites; (iii) the introduction of an empirical on-site Hubbard term correction on the Cu(3d) levels using the LDA+ U approach remedies some of the deficiencies of LDA and GGA (better spin localization and antiferromagnetic insulating ground state) but is not able to describe the charge-transfer nature of the insulating gap; and (iv) hybrid functionals including 20–25 % of nonlocal Fock exchange provide a satisfactory picture of the electronic structure of these materials including a proper description of the charge-transfer antiferromagnetic character of these materials and provide reliable estimates of the band gap and magnetic coupling constant.

DOI: [10.1103/PhysRevB.81.205123](https://doi.org/10.1103/PhysRevB.81.205123)

PACS number(s): 75.30.Et, 71.20.-b, 74.25.Jb

I. INTRODUCTION

The phenomenon of superconductivity was discovered almost 100 years ago¹ as a common property observed in many different types of pure metals and alloys. However, in 1986 a new class of superconducting materials of the family of ceramic perovskites based in La_2CuO_4 compound doped with Sr were discovered by Bednorz and Müller² exhibiting much higher critical temperatures than the superconductors known at that time, reaching almost 40 K and almost immediately the liquid-nitrogen temperature (77 K) in the related family of compounds based in $\text{YBa}_2\text{Cu}_3\text{O}_7$.³ The rise of the critical temperature found for these new materials, hereafter referred to as cuprates, reach the maximum established value of 135 K in the doped $\text{HgBa}_2\text{Ca}_2\text{Cu}_3\text{O}_{8+\delta}$ compound⁴ and up to 164 K under pressure.^{5,6} It is worth to point out that while the origin of superconductivity in metallic systems is explained by the standard phonon-mediated BCS theory, the origin of the superconducting phase in the doped cuprates, usually referred to as high- T_c superconductors (HTC), is still unknown.

Important features of HTC superconducting cuprates are a layered crystal structure with well-defined CuO_2 planes where it is widely accepted that injection of either holes or electrons results in the superconducting phase even if up to now there is no consensus on a general theory capable to describe the anomalous properties of the normal and superconducting phases of the doped materials and, hence, the underlying microscopic mechanism of HTC superconductivity remains unknown.^{7–9} The CuO_2 planes characteristic of HTC cuprates are separated by counterions packing the material and acting as pure ionic spectators. Other relevant properties of these compounds are a charge-transfer insulator character with a gap of ~ 2 eV arising from the mixing be-

tween O(2p) orbitals to Cu(3d) orbitals, a strong antiferromagnetic coupling between magnetic moments localized on the Cu^{2+} cations in the CuO_2 planes and a rich phase diagram as a function of doping and of the temperature. In fact, a minimum degree of doping is necessary to originate the superconductor phase.

From the large family of known cuprates, those containing well-separated Cu-O layers, hereafter referred to as monolayered cuprates, constitute the simplest structures to investigate the dominant electronic interactions in the CuO_2 planes and are chosen in the present work to investigate in detail their electronic structure using periodic models which go well beyond the standard local density approach (LDA) (Refs. 10 and 11) and generalized gradient approach (GGA) (Ref. 12) implementations of density functional theory (DFT). LDA and GGA methods have become standards for band-structure calculations and have proven to provide a very successful description of metals and hence to properly represent the electronic structure of metals and alloys, which are the main constituents of classical superconductors, but badly fail to describe the electronic structure of narrow band systems such as oxides, in general, and cuprates, in particular. In fact, LDA and GGA were among the first attempts to describe the electronic structure of HTC cuprates parent compounds, which were (incorrectly) predicted to have a metallic character hence raising a considerable expectation since this was a natural scenario for superconductivity to appear. Unfortunately, subsequent experimental work has unequivocally shown that these compounds are antiferromagnetic charge-transfer insulators (see above) and raising severe doubts on the adequacy of LDA and GGA to describe the electronic structure of these materials. The origin of the failure of LDA and GGA lies on the strong correlated nature of the electronic structure of these materials arising from the localized character of the Cu(3d) electrons and of their par-

ticular electronic structure with a local $3d^9$ configuration with an unpaired electron in the $d_{x^2-y^2}$ orbital. There is evidence that the strong electron-electron correlations that originate the strong antiferromagnetic coupling in the CuO_2 planes in the parent compounds is intimately related to the appearance of the superconducting state for a properly doped HTC cuprate.^{7,8,13,14}

The deficiency of LDA and GGA can be more or less efficiently remedied in several ways. On the one hand one can directly introduce a correction to the LDA or GGA potential by means of a Hubbard-type empirical U parameter giving rise to the so-called LDA+ U and GGA+ U methods.¹⁵ This empirical approach has been used as a simple and computationally efficient way to improve the LDA and GGA description of the electronic structure of strongly correlated systems such as reduced ceria^{16–18} or magnetic coupling in molecules.¹⁹ Alternatively, one can make use of the hybrid density functionals methods such as B3LYP (Refs. 20 and 21) which are very popular in quantum chemistry and increasingly used in condensed matter applications. Hybrid functionals provide a qualitatively correct description of the electronic structure of strongly correlated systems such as NiO,^{22,23} manganites,²⁴ and cuprates^{25–27} as shown by earlier studies using cluster models and local basis sets later corroborated by fully periodic calculations. The success of the hybrid functionals arises from the effect of mixing a fraction of nonlocal Fock exchange with the standard Slater local, or a suitable gradient corrected modification, exchange potential. This simple but efficient procedure allows one to predict the ground state of strongly correlated electronic systems. In particular, B3LYP has been tested for a large set of systems, from molecules to solids, providing a good description for some properties such as equilibrium geometries or vibrational frequencies in molecules and band gap of insulators and semiconductors although it appears to consistently overestimate the effective magnetic coupling parameter.²⁸ A further improvement of the B3LYP and similar hybrid functionals consist in exploiting the idea of range separation in the exchange-correlation functional which aim to fix the incorrect asymptotic behavior of LDA and GGA by introducing range separation into the exchange component of the potential. This idea has been recently developed and implemented by Scuseria *et al.*^{29,30} in different schemes and the Heyd, Scuseria, and Erzenhorf (HSE) short-range corrected hybrid functional³⁰ has been recently implemented in a periodic code using plane waves and proven to significantly improve the description of the electronic structure of strongly correlated oxides with respect to the qualitatively incorrect LDA (or GGA) description.^{31–36}

In the present work we use two different implementations of periodic hybrid density functional theory, one based in local atomic orbital and the other using a plane-wave-basis set, to describe the electronic structure and magnetic coupling in La_2CuO_4 and oxyhalide compounds such as $\text{Ca}_2\text{CuO}_2\text{Cl}_2$ and $\text{Sr}_2\text{CuO}_2\text{Cl}_2$ or $\text{Sr}_2\text{CuO}_2\text{F}_2$ which provide a representative series of monolayered cuprates where the relevant physics takes place essentially in the CuO_2 planes and, hence, constitute real systems which are closest to the simple models considering isolated CuO_2 only. We will show that the two approaches consistently predict these systems as an-

tiferromagnetic insulators with calculated values of the magnetic coupling constants close to experiment and provide a similar picture of the electronic structure, in particular, of the mixed charge-transfer character of the states near the Fermi level and evidencing once again the inadequacy of LDA and GGA to describe cuprates and similar magnetic oxides.

II. CRYSTAL STRUCTURE AND RELEVANT PROPERTIES OF MONOLAYERED CUPRATES

To study the electronic structure of monolayered HTC superconductor parent compounds by means of a periodic model, the knowledge of the crystal structure is required. This is because while present DF approaches, including the most accurate recently developed functionals, are able to provide relatively correct crystal structural parameters, they are not accurate enough to derive other properties very sensitive to small changes in the interatomic distances. This is because magnetic interactions in cuprates and other magnetic oxides are extremely sensitive to the interatomic distances,³⁷ a feature which is also reproduced by theoretical calculations.³⁸ Therefore, to avoid mixing effects arising from an incorrect crystal structure with those arising solely from the electronic structure, the experimental crystal structure is always used as an external input for the calculations. The set of monolayered cuprates studied in the present work includes the prototypal La_2CuO_4 compound as well as $\text{Ca}_2\text{CuO}_2\text{Cl}_2$, $\text{Sr}_2\text{CuO}_2\text{F}_2$, and $\text{Sr}_2\text{CuO}_2\text{Cl}_2$ which allow us to investigate the effect of the structure and composition in the magnetic coupling while maintaining the simple structure of well-separated CuO_2 planes. Note that the relevant part of the DOS around Fermi energy are essentially due to states originating from the CuO_2 planes and not from the remaining counterion planes. Moreover, their structure and electronic properties are well established from experiment and briefly described in the remaining part of this section.

La_2CuO_4 is no doubt among the most-studied superconducting parent compounds and was precisely the material that upon convenient doping led to the discovery of HTC superconductivity.² Doping this structure by Sr introduces holes in the CuO planes with $T_c=37$ K for $\text{La}_{2-x}\text{Sr}_x\text{CuO}_4$ with $x=0.15$.^{39,40} Holes are also introduced by an excess of oxygen leading to $\text{La}_2\text{CuO}_{4+\delta}$ with $T_c=40$ K for $\delta\sim 0.14$.⁴¹ At $T>530$ K, the crystallographic structure of La_2CuO_4 is tetragonal ($I4/mmm$) similar to the one shown in Fig. 1 whereas at lower T presents an orthorhombic distortion to the $Cmca$ (or $Bmab$) space group.⁴⁰ For simplicity, we consider study the tetragonal structure with crystal parameters extracted from experiment;⁴² $a=b=3.809$ Å, $c=13.169$ Å and with atoms at $\text{Cu}(0,0,0)$, $\text{O}_1(1/2,0,0)$, $\text{O}_2(0,0,0.182)$, and $\text{La}(0,0,0.362)$. This structure is characterized by well-separated CuO_2 planes, more than 6 Å distant from each other and with interleaved chemically inert LaO planes. This is the reason why simple models containing just one CuO_2 plane are customarily used in studies attempting to disclose the, yet unknown, physical mechanism of HTC superconductivity.⁷ Different experimental techniques show that La_2CuO_4 is a two-dimensional (2D) antiferromagnetic charge-transfer insulator with a gap of ~ 2.0 eV,⁴³ a Néel

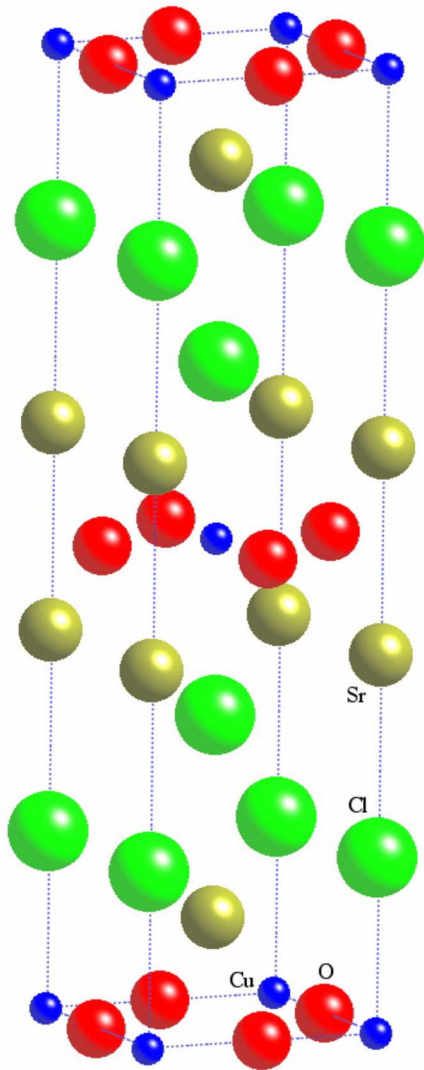


FIG. 1. (Color online) Schematic representation of the conventional unit cell of $\text{Sr}_2\text{CuO}_2\text{Cl}_2$ as representative of the family of monolayered cuprates studied in the present work.

temperature of 325 K and a magnetic moment per Cu between 0.1 and $0.5\mu_B$.⁴⁴ The magnetic order is dominated by a nearest-neighbor magnetic coupling constant of -146 ± 4 meV magnetic coupling parameter⁴⁵ established by high-resolution inelastic neutron scattering although earlier studies using similar techniques predicted smaller values ~ -135 meV.^{46,47}

$\text{Sr}_2\text{CuO}_2\text{Cl}_2$ has a structure very close to that of La_2CuO_4 at high temperature with Sr atoms instead of La and Cl atoms instead of axial O atoms. This compound shows a tetragonal $I4/mmm$ structure at all temperatures below the melting point and hence constitutes a prototype for cuprates with $a=b=3.972$, $c=15.613$ Å as axis and with atoms at $\text{Cu}(0,0,0)$, $\text{O}(1/2,0,0)$, $\text{Sr}(0,0,0.393)$, and $\text{Cl}(0,0,0.183)$.⁴⁸ This compound has not been found to exhibit a superconducting phase. The absence of superconducting transition in this compound is not motivated by an intrinsic limitation of its electronic structure but to the very high stability, derived from an extremely stable stoichiometry, which makes it very difficult to dope it.⁴⁸ It is considered in the present study

because is a representative system of single-layered superconductor cuprate parent compounds for which many different studies are available; see, for instance, discussion in Refs. 9 and 49. $\text{Sr}_2\text{CuO}_2\text{Cl}_2$ also exhibits a 2D antiferromagnetic insulator character with a charge-transfer gap about 1.9 eV with a slight dependence with temperature, a Néel temperature of 257 K with a magnetic moment $\sim 0.34\mu_B$ per Cu atom⁵¹ and a nearest-neighbor magnetic coupling constant of -125 ± 5 meV obtained from neutron-scattering experiments.^{46,50,51}

$\text{Sr}_2\text{CuO}_2\text{F}_2$ compound has been found to become superconducting after hole doping with excess fluorine ($\text{Sr}_2\text{CuO}_2\text{F}_{2+\delta}$ with $\delta \sim 0.6$, $T_c = 46$ K).⁵² Upon doping, the crystallographic structure becomes orthorhombic (space group $Fmmm$) related to that of $\text{Sr}_2\text{CuO}_2\text{Cl}_2$ in which F atoms replace Cl atoms. Because of this structural change, the cell parameters become $a=5.394$ Å, $b=5.513$ Å, and $c=13.468$ Å with atoms at $\text{Cu}(0,0,0)$, $\text{O}(1/4,1/4,0)$, $\text{F}(0,0,0.180)$, and $\text{Sr}(0,0,0.368)$. Note that now the conventional cell is twice the conventional cell of $\text{Sr}_2\text{CuO}_2\text{Cl}_2$. The experimental value for magnetic coupling parameter is not known due to the difficulty to prepare pure samples. The predicted value from accurate configuration interaction calculations is -140 meV.^{53,54} Experiment⁵² and theory^{53,54} evidence that its electronic-structure and magnetic properties are closely related to those $\text{Sr}_2\text{CuO}_2\text{Cl}_2$. Moreover, the closely related compound $\text{Sr}_{1.4}\text{Ba}_{0.6}\text{CuO}_2\text{F}_{2+\delta}$ is a *p*-type superconductor with $T_c \sim 64$ K, one of the highest-known critical temperatures for a monolayered HTC with the simple La_2CuO_4 structure.⁵⁵

Finally, $\text{Ca}_2\text{CuO}_2\text{Cl}_2$ is also very similar to $\text{Sr}_2\text{CuO}_2\text{Cl}_2$ with the only difference of Ca atoms instead of Sr and somewhat smaller cell parameters ($a=b=3.869$ Å and $c=15.05$ Å) and atoms at $\text{Cu}(0,0,0)$, $\text{O}(1/2,0,0)$, $\text{Ca}(0,0,0.396)$, $\text{Cl}(0,0,0.183)$ with tetragonal $I4/mmm$ structure).⁵⁶ It has been found to be a charge-transfer antiferromagnetic insulator ($T_N=250$ K) (Refs. 57 and 58) with an electronic structure similar to $\text{Sr}_2\text{CuO}_2\text{Cl}_2$.⁵⁹⁻⁶²

Before closing this brief summary of the most salient features of the four HTC superconductor cuprate parent compounds studied in the present work, it is important to point out that the apical O present in the La_2CuO_4 family is not an essential ingredient for the appearance of superconductivity (La_2CuO_4 vs $\text{Ca}_2\text{CuO}_2\text{Cl}_2$ and $\text{Sr}_2\text{CuO}_2\text{F}_2$) after doping although the interpretation of recent photoemission and extended x-ray absorption fine-structure spectroscopy experiments suggest that doping affects in a significantly different manner the original band structure of these parent compounds. Thus, in $\text{Ca}_2\text{CuO}_2\text{Cl}_2$ doping induces essentially a shift of the whole band structure whereas in La_2CuO_4 doping severely affects the valence and conduction bands and the presence of impurities affect the original charge-transfer insulating states.^{63,64} Therefore, a consistent description of the electronic and magnetic structure of the pure parent compounds seems to be a necessary requirement before attempting to understand the effect of doping on their electronic structure of cuprates. We must insist on the fact that the electronic structure of the parent compounds predicted by standard LDA and GGA approaches is qualitatively incorrect and thus useless to investigate the effect of doping. In the

forthcoming discussion we will show that the present hybrid density functional approaches provide such consistent description of the electronic structure of the undoped materials and constitute a promising step toward the description of the doped materials.

III. COMPUTATIONAL DETAILS

The electronic structure of monolayered cuprates has been investigated by means of periodic electronic band-structure calculations carried out in the framework of DFT using exchange-correlation potentials which go beyond the standard LDA and GGA methods. Two different well-established and broadly used implementations of DFT have been used which essentially differ in the basis set used to expand the density of the reference system of noninteracting electrons,^{65,66} i.e., within the well-known Kohn-Sham formalism. In the first case, the electron density of the system is described by means of a plane-wave- (PW) basis set whereas the second scheme considers uses a basis set consisting of Gaussian-type orbitals (GTO) centered on each atom and the final formalism is the periodic implementation of the linear combination of atomic orbitals approach.⁶⁷ Note that by construction the PW basis functions are delocalized over the entire system whereas the GTO are local functions aiming to represent atomic orbitals. For metals, where the electron density closely resembles the Fermi sea, PW basis functions seem an obvious choice whereas for oxides, and, in general, for systems where the electron density is well localized around the atoms, the GTO basis seems more appropriate. For sufficiently large basis sets, both PW and GTO must converge to the same result. We will present evidence that for the systems of interest in the present work, this is indeed the case.

Two different exchange-correlation models have been used which are the LDA+ U (Ref. 15) and various hybrid functionals. For the LDA+ U method, we follow the implementation of Anisimov¹⁵ and explore a broad range of U values between 5 and 9 eV with the main aim to establish the appropriate U value capable of reproducing the experimental values. In the case of hybrid functionals we use the standard B3LYP (Refs. 20 and 21) method as well as the recently developed short-range corrected hybrid functional proposed by HSE (Ref. 30) which among other benefits exhibits a better convergence toward the variational energy when a PW basis set is used. This is because this functional is capable to avoid the convergence problem associated with the slow potential decay represented by $-c/r$ for all hybrid functionals instead of the correct Coulomb potential $-1/r$. The HSE06 functional mixes 25% of the exact nonlocal Fock exchange potential with the pure Perdew-Burke-Ernzerhof⁶⁸ (PBE) exchange correlation GGA functional and uses a short-range component for nonlocal part selected by the ω screening parameter which was chosen to be a 0.2 \AA^{-1} to conform with the HSE06 definition.³² The PBE0 method⁶⁹ [or PBE1PBE (Ref. 70)], which is a limiting case of HSE06 when the screening parameter ω defining the range separation tends to zero, has been also considered. Note that PBE0 (and also B3LYP) represents a considerable improvement over LDA

and GGA for the description of thermochemistry, equilibrium geometries, and vibrational frequencies of molecules.^{71,72} The LDA+ U and HSE06 calculations have been carried out using a PW basis set to describe the valence electrons (see below) with the effect of the nuclei and core electron on the valence density taken into account using the projector-augmented-wave (PAW) (Refs. 73 and 74) method as implemented in the VASP code^{75,76} whereas B3LYP and PBE0 calculations have been carried out using the CRYSTAL06 package⁷⁷ with atomic GTO basis sets which are described below. For La_2CuO_4 and $\text{Ca}_2\text{CuO}_2\text{Cl}_2$ cases, PBE0 calculations have been also carried out using the PW basis set. This permits a direct comparison between calculations obtained with the different basis sets and provides compelling evidence that in each case the basis set is large enough so as to consider the energy differences of interest in the present work (see next section) essentially converged with respect to basis set size. Finally, pure GGA calculations with the PBE functional, which is the limit of HSE06 when the ω parameter approaches infinity, have been carried out for all compounds always predicting the incorrect metallic ground state. Some representative cases will be included in the discussion to illustrate once again the failure of pure DFT approaches to describe the electronic structure of these strongly correlated systems.

For the LDA+ U , the PAW chosen leave Cu with 17 electrons [$3p^6, 3d^{10}, 4s^1$], O with six electrons [$2s^2, 2p^4$], La with nine electrons [$5p^6, 5d^1, 6s^2$], Sr with ten electrons [$4s^2, 4p^6, 5s^2$], Cl with seven electrons [$3s^2, 3p^5$], F with seven electrons [$2s^2, 2p^5$], and Ca with eight electrons [$3p^6, 4s^2$]. Due to the large computational requirements of the hybrid HSE06, and even larger for PBE0, calculations carried out with the PW basis set it is necessary to use a larger core for Cu and Ca leaving 11 [$3d^{10}, 4s^1$] and two [$4s^2$] valence electrons, respectively. For the B3LYP and PBE0 hybrid DF calculations carried out with GTO basis sets and the CRYSTAL code we use standard Gaussian basis sets which explicitly consider all electrons for Cu, O, F, La, and Ca whereas Hay and Wadt effective core potentials⁷⁸ are used to describe the cores of Sr and Cl. These GTO basis sets have been optimized for the corresponding ions and the outer isolated sp or sp and d exponents have been reoptimized for a given environment.⁷⁹ A shrinking factor of 4 has been adopted for forming a regular reciprocal with 21 k points in the irreducible Brillouin zone, we also adopt 7,7,7,7 and 14 as the integral tolerances (ITOL1–5) to obtain a good precision in mono-electronic and bi-electronic integrals. The total energy convergence threshold exponent was set to 6. In all cases, PW and GTO calculations, appropriate supercells were built in order to calculate the necessary antiferromagnetic phases. It is worth pointing out that in the PW calculations one uses the conventional unit cell whereas the primitive unit cell is used in the GTO calculations. For a more detailed discussion the reader is referred to our recent work in Ref. 80.

IV. MODELING MAGNETIC INTERACTIONS

Magnetic interactions represent an important ingredient, which seems to be a crucial factor in triggering superconduc-

tivity in HTC cuprates.^{43,81,82} The low-energy spectrum of these systems is essentially due to spin excitations of the AF ground state and, hence, it is possible to argue that the corresponding physics can be fully explained by making use of a model or effective Hamiltonians which explicitly act on the spin part of the wave function. In the case of cuprates, the low-energy spectrum is dominated by the interactions between localized spin moments of magnitude $S=1/2$ (arising from unpaired electrons localized in Cu ions) and is generally described by means of spin Hamiltonians among which the simplest one contains two-body operators only and gives rise to the well-known Heisenberg-Dirac-Van Vleck Hamiltonian (\hat{H}^{HDVV}) as in Eq. (1)

$$\hat{H}^{HDVV} = - \sum_{i,j} J_{ij} \hat{S}_i \hat{S}_j, \quad (1)$$

where J_{ij} is the magnetic coupling constant between i and j sites with S_i and S_j total effective spin operators. Here, it is important to point out that whereas the overall picture can be qualitatively described by taking into account two body terms only, a detailed description of the low-energy spectrum requires including higher-order terms. In particular, recent experiments^{45,83} and theoretical hybrid DF calculations (hence going beyond the standard LDA and GGA methods) provide compelling evidence of the importance of cyclic four-body terms.^{84,85} Nevertheless, there is also strong evidence that nearest-neighbor two-body interactions are enough to obtain reliable predictions of the magnetic coupling constant J ⁸⁶ which indeed is related to the final T_c in the doped system.⁸¹ Mapping the low-energy electronic states of the exact and spin Hamiltonians allows one to relate the magnitude of the magnetic coupling constant to total-energy differences between appropriate spin states of Eq. (1).²⁸ However, for periodic system it is not always possible to handle pure spin states and one has necessarily to rely on appropriate mappings between the low-lying magnetic solutions, typically ferromagnetic (FM) and the possible antiferromagnetic (AF) solutions, obtained by means of periodic DF calculations in the appropriate unit cell and those of the Ising Hamiltonian in Eq. (2); a simplification of the Heisenberg-Dirac-Van Vleck Hamiltonian in Eq. (1) which only commutes with the z component of the total spin operator.

$$H^{\text{Ising}} = - \sum_{i,j} J_{ij} \hat{S}_{z_i} \hat{S}_{z_j}. \quad (2)$$

In such a case it is easy to show⁸⁰ that

$$E(\text{AF}_I) - E(\text{FM}) = - N_I k_I J_{ij} S_{z_i}^2, \quad (3)$$

where the subindex I refers to one of the possible AF solutions, N_I is the number of magnetic centers on the cell, k_I is the number of equivalent ij neighbor magnetic centers of a given magnetic center, and S_z is the z component of total spin per center. Since in the periodic calculations one is forced to use a single Slater determinant and to seek for the best variational solution for such a trial wave function or density it is possible to map the expectation value of the Heisenberg and of the exact Hamiltonians for the FM and AF _{I} solutions

which allows one to prove that the J_{ij} parameter in Eqs. (1) and (2) is the same,²⁸ thus validating the present approach.

In the case of the single-layered cuprates studied in the present work, the magnetic behavior may be described as a quasi-two-dimensional magnetic system arising from the square net of $S=1/2$ localized spin moments associated to the d^9 atomic configuration of the Cu^{2+} ions. The J_{ij} values obtained from calculations can be related to their experimental counterparts derived from statistical mechanics expressions connecting macroscopic properties such as magnetic susceptibility or heat capacity and its temperature dependence, or spin-polarized neutron-diffraction data. The agreement between calculated and experimental values being excellent provided the right exchange-correlation functional is used in the periodic calculations²⁵⁻²⁷ or through appropriate configuration interaction cluster model calculations.^{54,81,86} In the present context, the magnitude of the J parameter can be used as a sensitive property to test the accuracy and reliability of the different electronic-structure methods or, as in the case of LDA+ U , as an additional calibration property.

V. RESULTS AND DISCUSSION

A. Failure of LDA and GGA to describe the ground-state properties of cuprates

We already mentioned that LDA and GGA fail to describe the antiferromagnetic insulating character of the ground state of monolayered cuprates. This failure occurs for all implementations of GGA (PW91 or PBE) as illustrated by the density of states (DOS) plots of $\text{Sr}_2\text{CuO}_2\text{Cl}_2$ and La_2CuO_4 (Fig. 2) obtained for the antiferromagnetic ground state from periodic DF calculations using a plane-wave-basis set. These DOS plot predict a metallic behavior for these two superconductor cuprates parent compounds and evidence the lack of spin localization, in clear contradiction to experimental evidence.^{61,87} Calculations using the same PBE exchange-correlation potential and a localized GTO basis set lead to the same picture (not shown). The atom projected DOS in Fig. 2 show that, in addition to the incorrect metallic picture, these calculations suggest a too small degree of hybridization between Cu(3d) and O(2p) and exceedingly small spin densities at the Cu sites, again both in clear contradiction to experiment. The LDA and GGA calculations for the rest of compounds follow the same trend and consequently will not be further discussed. The complete set of results is, however, available upon request to the authors.

B. Effect of the on-site U Hubbard term: LDA+ U and GGA+ U

Inclusion a U term in the Cu(3d) states strongly modifies the electronic density leading to a density of states and to spin density at the Cu sites which as we will show in the following discussion and contrarily to the results described in the previous section for the LDA and GGA formalisms, is in qualitative agreement with experiment. However, this approach is not free of problems since it modifies only the relative energy of the Cu(3d) states and hence cannot account for the rather large degree of hybridization between

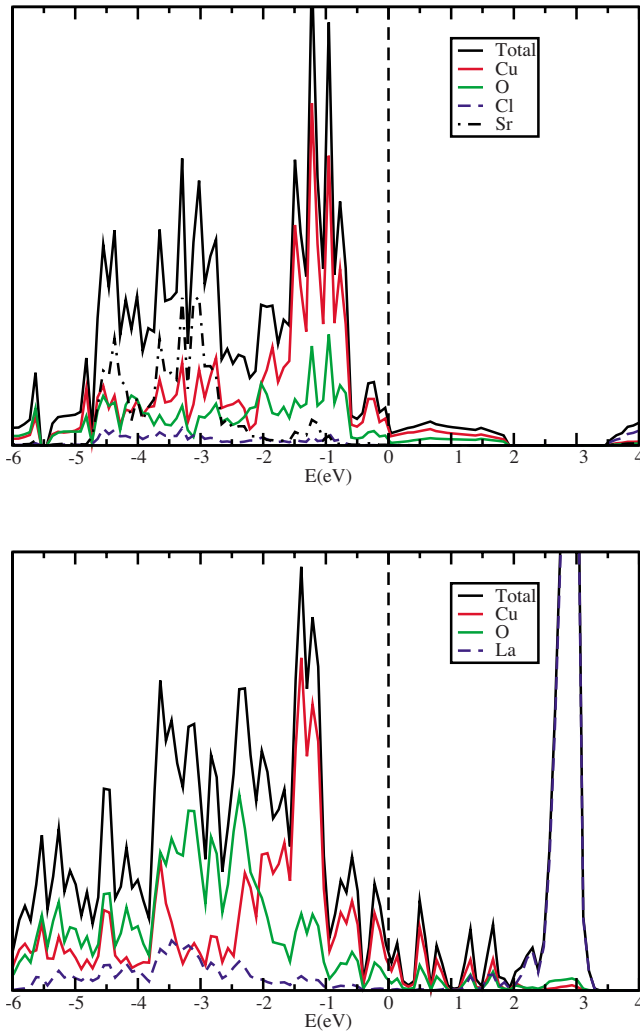


FIG. 2. (Color online) Density of states for the calculated anti-ferromagnetic ground-state solutions of $\text{Sr}_2\text{CuO}_2\text{Cl}_2$ (top) and La_2CuO_4 (bottom) cuprate as obtained from periodic density functional calculations using a plane-wave-basis set and the PBE functional.

$\text{Cu}(3d)$ and $\text{O}(2p)$ states. In this sense, the $\text{LDA}+U$ and $\text{GGA}+U$ methods provide a partial remedy to the deficiency of the original LDA and GGA ones. In fact, it is well established that doping with holes strongly affects the occupation of the $\text{O}(2p)$ band whereas this is almost unaffected by the U correction in the $\text{Cu}(3d)$ states. A final problem with this type of approach is the choice of the U value. In the present work we have decided to follow the strategy followed by Loschen *et al.* to describe CeO_2 and Ce_2O_3 (Ref. 18) and to describe magnetic coupling in molecular systems within the $\text{LDA}+U$ and $\text{GGA}+U$ approaches.¹⁹ To this end we calibrated the $\text{LDA}+U$ methodology against experiment using two different well-defined properties: the band gap and the magnetic coupling constant J . Figure 3 summarizes the results of this calibration and evidence the difficulty to find a U value which simultaneously describes these two important properties. For all investigated cuprates, the band-gap energy increases monotonically with U whereas for the magnetic coupling constant the dependence is more complex and less

obvious. In any case, results in Fig. 3 suggest that a value of $U=8$ eV provides a good compromise. Note that this is larger than the value of $U=6-7$ eV suggested in previous work on similar systems but focusing in the band gap only.⁸⁸ Therefore, calibration with more than one property seems to be a necessary requirement to provide a meaningful physical picture and reliable predictions. In the following we will discuss the results for whole set of cuprates obtained with $\text{LDA}+U$ and $U=8$ eV.

Table I summarizes the main results obtained in the present work and evidences the excellent agreement between $\text{LDA}+U$ and experimental values for the band gap (Δ) and for the magnetic coupling constant J . However, one must advert that such agreement is the result of the procedure used to select the Hubbard correction term U . Nevertheless, these results show that tuning the U parameter enables one to reach a reasonable picture of the electronic structure of these monolayered cuprates. The picture is not completely satisfactory because the U term affects directly the $\text{Cu}(3d)$ levels, the rest of one electron states being modified only in response to energy position of the $\text{Cu}(3d)$ levels. A consequence of this picture of the electronic structure is an incorrect description of the $\text{Cu}(3d)\text{-O}(2p)$ hybridization which is evident from the experiments.^{51,61,87} This is clear from calculated density of states of these systems reported in Fig. 4 which even showing a clear band-gap evidence that the $\text{O}(2p)$ contribution to the states near the top of the valence band is too large. This is due to the excessive delocalization of the electron density predicted by the LDA functional (Fig. 2) which is not remedied by the inclusion of a U term in the $\text{Cu}(3d)$ states. Of course, this deficiency of $\text{LDA}+U$ makes the description of doping in these systems difficult and claims for a more accurate treatment. It is also important to stress the localized character of the charge and spin density on these systems as predicted by the $\text{LDA}+U$ method. Results in Table II report the calculated spin density at the Cu sites for the FM and AF solutions as obtained from a Bader analysis of the charge density.⁸⁹ The description is consistent with a highly ionic character and evidence that the spin densities are almost independent of the magnetic solution thus validating the assumption of a Heisenberg spin Hamiltonian to extract the magnetic constants.

C. Hybrid density functional description of the ground-state properties of cuprates

Periodic calculations using the PBE0 functional for La_2CuO_4 and $\text{Ca}_2\text{CuO}_2\text{Cl}_2$ using GTO and PW basis set allow a direct estimate of the effect of the basis set on the calculated properties of interest. This is a necessary step because, mainly for historical reasons, most of the periodic hybrid DF calculations reported in the literature use the B3LYP potential when in connection with a GTO basis set whereas the HSE06 potential is the usual choice when using a PW basis set. For La_2CuO_4 and $\text{Ca}_2\text{CuO}_2\text{Cl}_2$, the DOS arising from PBE0 calculations using either GTO or PW basis sets are very similar but with some difference in the predicted band gap value. Thus, for La_2CuO_4 one finds 4.2 eV (PBE0 and GTO) and 3.8 eV (PBE0 and PW) whereas for

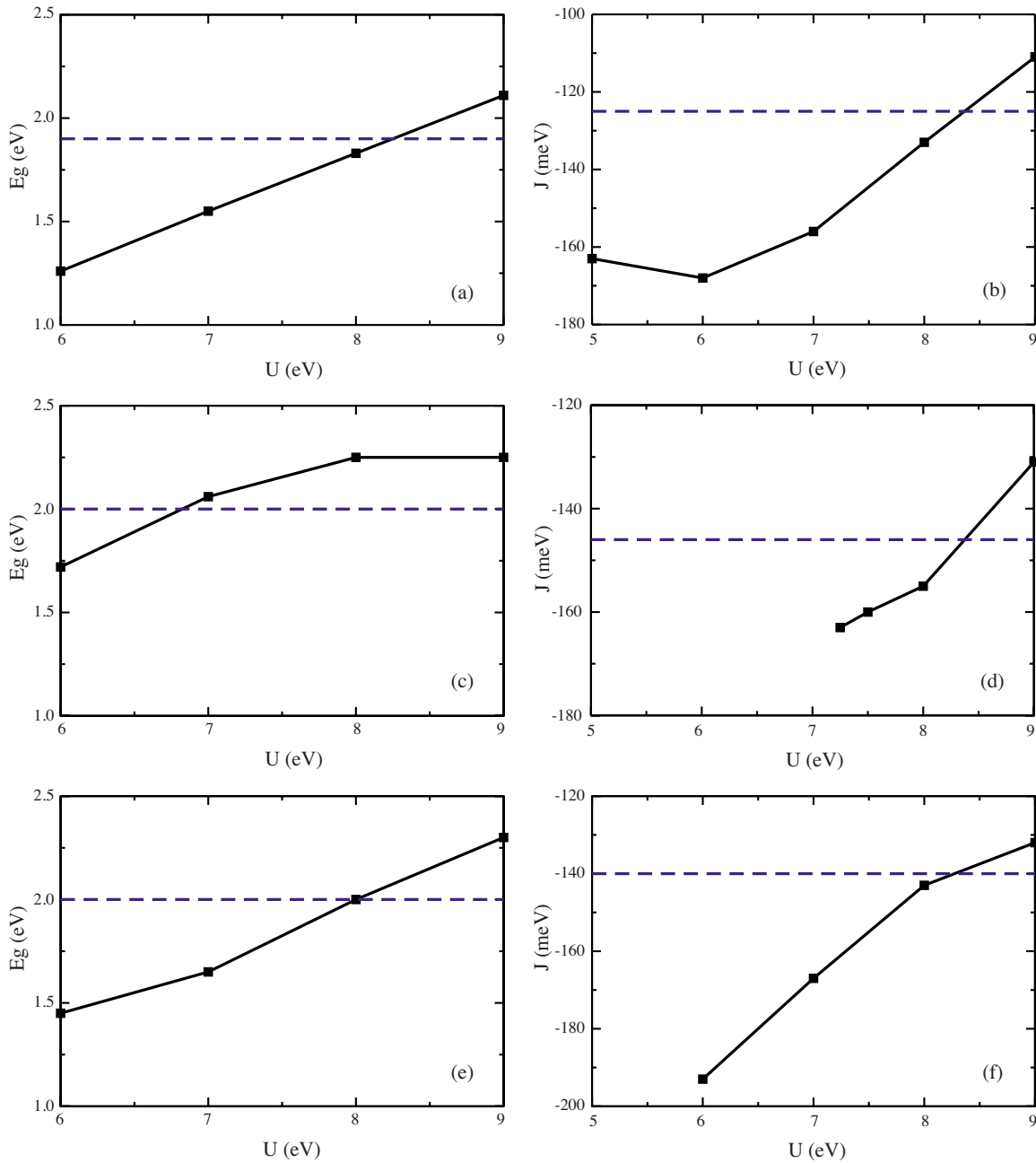


FIG. 3. (Color online) Band gap values (E_g , left panels) and magnetic coupling constant (J , right panels) of [(a) and (b)] Sr₂CuO₂Cl₂, [(c) and (d)] La₂CuO₄, and [(e) and (f)] Ca₂CuO₂Cl₂ as obtained from periodic density functional calculations using the LDA+ U methods as a function of U . For U values below 6–7 eV, Ca₂CuO₂Cl₂ and La₂CuO₄ show an unphysical antiferromagnetic ground state with very poor spin localization (i.e., nonmagnetic, closed shell in nature) leading to exceedingly large J values. The horizontal dashed line indicates the experimental values for Sr₂CuO₂Cl₂ and La₂CuO₄ whereas for Ca₂CuO₂Cl₂ refer to results from accurate embedded cluster model configuration interaction calculations (Ref. 54).

Ca₂CuO₂Cl₂ the calculated values are 3.8 and 3.3 eV, respectively. The effect of the basis set is noticeable and, in principle, the PW basis set is more complete. Nevertheless, the predicted band-gap values are reasonable and constitute an improvement over LDA and GGA. Interestingly, the calculated values of the magnetic coupling constants and spin densities at the Cu sites in the AF ground state are even more similar: for La₂CuO₄ one finds $J=-154$ meV (PBE0 and GTO) and -182 meV (PBE0 and PW) whereas for Ca₂CuO₂Cl₂ the corresponding values are -171 and

-192 meV, respectively. Similarly, the spin densities at the Cu site for La₂CuO₄ are 0.70 (PBE0 and GTO) and 0.64 (PBE0 and PW) and 0.67 and 0.61, respectively, for Ca₂CuO₂Cl₂. From this set of calculations it is clear that the effect of the basis set on the calculated values of these properties is $\sim 10-15\%$, a quantity which can be even reduced by increasing the quality of the GTO basis set and the energy cutoff for the plane waves. However, except for values fully converged with respect to the basis set (i.e., the so-called basis set limit) it is very difficult to assess which of the two

TABLE I. Calculated values for the band gap (Δ in eV) and magnetic coupling constant (J in meV) of monolayered cuprates as obtained from density functional calculations using the LDA+ U ($U=8$ eV), B3LYP and HSE06 exchange-correlation potential. Experimental values are also included for comparison.

Property	Compound	LDA+ U	B3LYP	HSE06	Experimental
Δ	Sr ₂ CuO ₂ Cl ₂	1.8	2.6	2.0	1.9
	Ca ₂ CuO ₂ Cl ₂	2.0	2.8	2.3	
	La ₂ CuO ₄	2.3	3.1	2.5	2.0
	Sr ₂ CuO ₂ F ₂	2.0	2.7	2.5	
J	Sr ₂ CuO ₂ Cl ₂	-133	-180	-182	-125
	Ca ₂ CuO ₂ Cl ₂	-143	-198	-192	
	La ₂ CuO ₄	-155	-183	-187	-146
	Sr ₂ CuO ₂ F ₂	-152	-206	-198	-140 ^a

^aResults from embedded cluster model configuration interaction calculations in Ref. 54.

basis set is more complete. The important message is therefore that very different computational schemes provide essentially the same results, within 10%, when using the same exchange-correlation functional. Note also that in the PBE0 calculations carried out with the GTO basis set all electrons in the Cu-O planes are explicitly considered whereas the approximate PAW description of the atomic cores is used in the PBE0 plane-wave calculations.^{90,91}

Next, we discuss results for the whole series of monolayered cuprates considered in the present work as predicted by the B3LYP and HSE06 hybrid exchange-correlation potentials which have become the standard choice in periodic hybrid DF calculations using GTO and PW basis sets, respectively. The full set of results reported in Table I indicates that the two approaches are qualitatively correct, predicting an insulating state for these undoped cuprates although the numerical agreement with the experimental values of Δ and J is not as good as in the case of the LDA+ U method. A better numerical agreement can be found by tuning the amount of nonlocal Fock exchange although this may be different for Δ and J and, in addition, introduces an unnecessary additional degree of empiricism. In any case, the results from hybrid density functional in Table I deserve some additional comments. First, we note the coherent description of both B3LYP and HSE06 that is to be expected from the fact that both contain a similar amount ($\sim 25\%$) of Fock exchange and this is by far the dominant correction to LDA or GGA.^{22,92} Finally, the differences between the HSE06 results reported in Table I for La₂CuO₄ and Ca₂CuO₂Cl₂ and the PBE0 ones, both obtained with the same basis sets, merit an additional comment. The HSE06 and PBE0 functionals differ only in the treatment of the Fock exchange, both contain 25% of Fock exchange but in the HSE06 this is screened in short-range electron-electron distance whereas in the PBE0 it is kept always fixed. The effect of range separation is noticeable for the calculated band gap, which for both cuprates is roughly reduced by 0.7 eV when going from PBE0 to HSE06. This is exactly the expected trend since HSE06 screens the Fock potential in a region of space and necessarily has to produce results between PBE0 and the pure GGA PBE potential. This effect is not found when analyzing the calculated magnetic coupling where PBE0 and HSE06 value differ by less than 5 meV. This is also to be expected because

the magnetic coupling constant is a local property whereas the band gap is a property of the whole solid.

Additional information about the chemical bonding in this cuprates is provided by the charge distribution on the different planes present in the structure. The charge distribution per formula unit of the different compounds obtained from Mulliken (B3LYP and GTO) and Bader analysis (HSE06 and PW) are summarized as follows: For La₂CuO₄ one has [CuO₂]^{-1.86} [La₂O₂]^{+1.86} from B3LYP; [CuO₂]^{-1.50} [La₂O₂]^{+1.50} from HSE06, and [CuO₂]^{-1.42} [La₂O₂]^{+1.42} from LDA+ U . For Ca₂CuO₂Cl₂ the corresponding values are [CuO₂]^{-1.96} [Ca₂Cl₂]^{+1.96}, [CuO₂]^{-1.94} [Ca₂Cl₂]^{+1.94}, and [CuO₂]^{-1.52} [Ca₂Cl₂]^{+1.52} from B3LYP, HSE06, and LDA+ U , respectively. For each method, the calculated values for Sr₂CuO₂Cl₂ and Sr₂CuO₂F₂ are very similar to those obtained for Ca₂CuO₂Cl₂ and will not be further commented. The results above evidence the large ionicity of these compounds and indicate that this is larger for Ca₂CuO₂Cl₂ than for La₂CuO₄ and confirm the exceedingly large charge (and spin) delocalization predicted by the LDA+ U .

A second pertinent comment concerns the picture of the electronic structure arising from the hybrid density functional calculations. Here, the inclusion of a fraction of non-local Fock exchange affects the whole electronic structure and, as a result, the Cu(3*d*)-O(2*p*) hybridization on the states near the top of the valence band is now well described. This will be discussed in detail below when describing the calculated density of states of these systems. A third final comment concerns the similarities and difference for the calculated Δ and J values. For the latter, B3LYP and HSE06 predict almost the same numerical values whereas for the former the differences are slightly larger. The better agreement for the J values comes from the fact that this property is obtained by a difference of total energy for two different magnetic solutions whereas Δ depends on the description of the band structure and this is more sensitive to the basis set differences. In particular, the better agreement between HSE06 and experimental values has to be attributed to the better completeness of the plane-wave-basis set. On the other hand, the agreement between B3LYP and HSE06 calculated J values is consistent with the calculated spin density at the Cu sites for the FM and AF reported in Table II. The B3LYP values have been obtained from a Mulliken analysis whereas

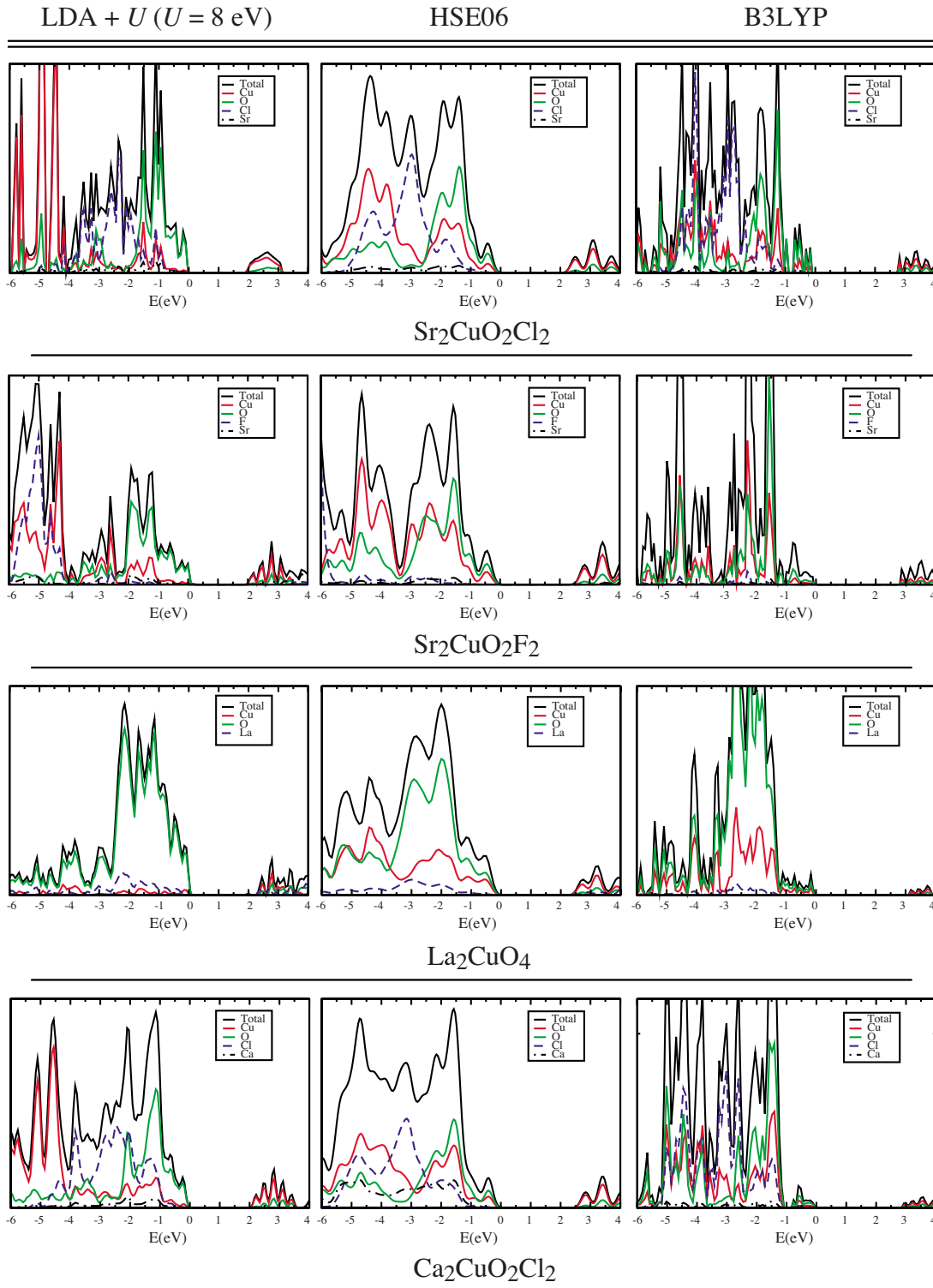


FIG. 4. (Color online) Density of states of antiferromagnetic ground state for LDA+ U ($U=8$ eV), B3LYP and HSE06 functional, calculated for all compounds in the present work.

in the case of the HSE06 they have been obtained from a Bader analysis of the charge density as in the case of LDA+ U values described above. Again, the description is consistent with a highly ionic character leading to spin densities localized at the Cu sites.

Finally, let us discuss the picture of the electronic structure of these cuprates emerging from the HSE06 and B3LYP

hybrid exchange-correlation potentials. The density of states reported in Fig. 4 for these two functionals is very similar, as expected from the fact that both functionals contain a similar amount (25% and 21%) of nonlocal Fock exchange respectively. Taking into account that the two series of calculations use very different basis sets (plane wave and localized GTO, respectively), the similarity is remarkable and indicates the

TABLE II. Calculated spin density at Cu sites in the AF and FM solutions as derived from Bader (LDA+ U and HSE06) and Mulliken (B3LYP) analysis in the different systems considered in the present work.

Compound	LDA+ U		B3LYP		HSE06	
	AF	FM	AF	FM	AF	FM
Sr ₂ CuO ₂ Cl ₂	0.68	0.78	0.62	0.68	0.63	0.74
Ca ₂ CuO ₂ Cl ₂	0.67	0.78	0.62	0.70	0.60	0.74
La ₂ CuO ₄	0.68	0.79	0.66	0.72	0.62	0.76
Sr ₂ CuO ₂ F ₂	0.68	0.78	0.62	0.69	0.60	0.75

maturity of the methods and of their numerical implementation. Both, HSE06 and B3LYP properly describe these cuprates as antiferromagnetic insulators (Tables I and II) and, in addition, reveal a noticeably large degree of hybridization between Cu(3d) and O(2p) states near the top of the valence band indicating that, in addition to the correct description of these systems as insulators, the insulating gap is of charge transfer nature.

VI. CONCLUSIONS

The ability of current density functional methods to describe the electronic and magnetic structure of a series of monolayered high- T_c superconducting cuprate parent compounds is investigated by means of periodic representation of the materials. The study of the electronic structure, band gap, density of states, and magnetic coupling reveals that: (1) LDA and GGA predict a metallic ground state with a very poor spin density at Cu sites and characterized by an exceedingly large delocalization of the electron density which is in contradiction to experimental evidence describing these systems as charge-transfer antiferromagnetic insulators with spin density localized mainly at the Cu sites. (2) Introduction of an on-site Hubbard term correction on the Cu(3d) levels remedies some of the deficiencies of LDA and GGA. It properly describes the systems as antiferromagnetic insulators but is not able to describe the charge-transfer nature of the insulating gap. Furthermore, the calculated results for the band gap and the magnetic coupling constant strongly depend on the value of U chosen. Comparison to available experimental data suggests that $U=8$ eV is an optimum value. (3) For a given hybrid exchange-correlation potential such as PBE0,

consistent results are found independently of the basis set used (GTO or PW) although this may affect the calculated values of the band gap and magnetic coupling constants by at most 10%. (4) Hybrid functionals, either HSE06 or B3LYP, provide a satisfactory picture of the electronic structure of these materials including a proper description of the charge-transfer antiferromagnetic character of these materials and provide reliable estimates of the band gap and magnetic coupling constant. (5) The good agreement between the HSE06 calculations carried out employing a plane-wave-basis set and the B3LYP results arising from a basis set of atomic orbitals represented by local Gaussian-type orbitals indicates that these approaches have reached the necessary degree of coherence to permit direct comparisons. (6) Finally, it is worth to point out that the periodic implementation of hybrid density functional theory-based methods represents nowadays the only way to describe in practice the electronic structure and properties of these type of systems in a sufficiently accurate way although one must admit that they suffer from the choice of the amount of nonlocal Fock exchange which still represents an external input.

ACKNOWLEDGMENTS

P.R. thanks the Spanish *Ministerio de Ciencia e Innovación* (MICINN) for a predoctoral grant. Financial support has been provided by Spanish MICINN (Grant No. FIS2008-02238/FIS) and in part Generalitat de Catalunya (Grant No. 2009SGR1041 and XRQTC). Computational time has been generously provided by the *Centre de Supercomputació de Catalunya* (CESCA) and Barcelona Supercomputing Center (BSC).

¹H. Kamerling Onnes, *Comm. Phys. Lab. Univ. Leiden* **119** (1911); **120** (1911); **122** (1911); **124** (1911).

²J. G. Bednorz and K. A. Müller, *Z. Phys. B* **64**, 189 (1986).

³M. K. Wu, J. R. Ashburn, C. J. Torng, P. H. Hor, R. L. Meng, L. Gao, Z. J. Huang, Y. Q. Wang, and C. W. Chu, *Phys. Rev. Lett.* **58**, 908 (1987).

⁴A. Schilling, M. Cantoni, J. D. Guo, and H. R. Ott, *Nature (London)* **363**, 56 (1993).

⁵A. R. Armstrong, W. I. F. David, I. Gameson, P. P. Edwards, J. J.

Capponi, P. Bordet, and M. Marezio, *Phys. Rev. B* **52**, 15551 (1995).

⁶L. Gao, Y. Y. Xue, F. Chen, Q. Xiong, R. L. Meng, D. Ramírez, C. W. Chu, J. H. Eggert, and H. K. Mao, *Phys. Rev. B* **50**, 4260 (1994).

⁷E. Dagotto, *Rev. Mod. Phys.* **66**, 763 (1994).

⁸M. R. Norman and C. Pepin, *Rep. Prog. Phys.* **66**, 1547 (2003).

⁹A. Damascelli, Z. Hussain, and Z.-X. Shen, *Rev. Mod. Phys.* **75**, 473 (2003).

- ¹⁰S. H. Vosko, L. Wilk, and M. Nusair, *Can. J. Phys.* **58**, 1200 (1980).
- ¹¹J. P. Perdew and A. Zunger, *Phys. Rev. B* **23**, 5048 (1981).
- ¹²J. P. Perdew, J. A. Chevary, S. H. Vosko, K. A. Jackson, M. R. Pederson, D. J. Singh, and C. Fiolhais, *Phys. Rev. B* **46**, 6671 (1992).
- ¹³P. W. Anderson, *Low Temp. Phys.* **32**, 282 (2006).
- ¹⁴P. W. Anderson, *Science* **316**, 1705 (2007).
- ¹⁵V. I. Anisimov, M. A. Korotin, J. A. Zaanen, and O. K. Andersen, *Phys. Rev. Lett.* **68**, 345 (1992).
- ¹⁶M. Nolan, S. Grigoleit, D. C. Sayle, S. C. Parker, and G. W. Watson, *Surf. Sci.* **576**, 217 (2005).
- ¹⁷C. W. M. Castleton, J. Kullgren, and K. Hermansson, *J. Chem. Phys.* **127**, 244704 (2007).
- ¹⁸C. Loschen, J. Carrasco, K. M. Neyman, and F. Illas, *Phys. Rev. B* **75**, 035115 (2007).
- ¹⁹P. Rivero, C. Loschen, I. de P. R. Moreira, and F. Illas, *J. Comput. Chem.* **30**, 2316 (2009).
- ²⁰A. D. Becke, *J. Chem. Phys.* **98**, 5648 (1993).
- ²¹C. Lee, W. Yang, and R. G. Parr, *Phys. Rev. B* **37**, 785 (1988).
- ²²I. de P. R. Moreira, F. Illas, and R. L. Martin, *Phys. Rev. B* **65**, 155102 (2002).
- ²³X. B. Feng and N. M. Harrison, *Phys. Rev. B* **69**, 035114 (2004).
- ²⁴D. Muñoz, N. M. Harrison, and F. Illas, *Phys. Rev. B* **69**, 085115 (2004).
- ²⁵J. K. Perry, J. Tahir-Kheli, and W. A. Goddard, *Phys. Rev. B* **63**, 144510 (2001).
- ²⁶X. Feng and N. M. Harrison, *Phys. Rev. B* **70**, 092402 (2004).
- ²⁷I. de P. R. Moreira and R. Dovesi, *Int. J. Quantum Chem.* **99**, 805 (2004).
- ²⁸I. de P. R. Moreira and F. Illas, *Phys. Chem. Chem. Phys.* **8**, 1645 (2006).
- ²⁹O. A. Vydrov and G. E. Scuseria, *J. Chem. Phys.* **125**, 234109 (2006).
- ³⁰J. Heyd, G. E. Scuseria, and M. Ernzerhof, *J. Chem. Phys.* **118**, 8207 (2003); **124**, 219906(E) (2006).
- ³¹J. Heyd and G. E. Scuseria, *J. Chem. Phys.* **120**, 7274 (2004).
- ³²J. Heyd and G. E. Scuseria, *J. Chem. Phys.* **121**, 1187 (2004).
- ³³J. Heyd, J. E. Peralta, G. E. Scuseria, and R. L. Martin, *J. Chem. Phys.* **123**, 174101 (2005).
- ³⁴J. E. Peralta, J. Heyd, G. E. Scuseria, and R. L. Martin, *Phys. Rev. B* **74**, 073101 (2006).
- ³⁵P. J. Hay, R. L. Martin, J. Uddin, and G. E. Scuseria, *J. Chem. Phys.* **125**, 034712 (2006).
- ³⁶P. Rivero, I. de P. R. Moreira, G. E. Scuseria, and F. Illas, *Phys. Rev. B* **79**, 245129 (2009).
- ³⁷M. C. Aronson, S. B. Dierker, B. S. Dennis, S. W. Cheong, and Z. Fisk, *Phys. Rev. B* **44**, 4657 (1991).
- ³⁸J. Casanovas, J. Rubio, and F. Illas, *Phys. Rev. B* **53**, 945 (1996).
- ³⁹R. J. Cava, A. Santoro, D. W. Johnson, Jr., and W. W. Rhodes, *Phys. Rev. B* **35**, 6716 (1987).
- ⁴⁰P. G. Radaelli, D. G. Hinks, A. W. Mitchell, B. A. Hunter, J. L. Wagner, B. Dabrowski, K. G. Vandervoort, H. K. Viswanathan, and J. D. Jorgensen, *Phys. Rev. B* **49**, 4163 (1994).
- ⁴¹H. H. Feng, Z. G. Li, P. H. Hor, S. Bhavaraju, J. F. DiCarlo, and A. J. Jacobson, *Phys. Rev. B* **51**, 16499 (1995).
- ⁴²J. M. Longo and P. H. Raccach, *J. Solid State Chem.* **6**, 526 (1973).
- ⁴³*Handbook of High-Temperature Superconductivity*, edited by J. R. Schrieffer and J. S. Brooks (Springer-Verlag, New York, 2007).
- ⁴⁴W. E. Pickett, *Rev. Mod. Phys.* **61**, 433 (1989).
- ⁴⁵R. Coldea, S. M. Hayden, G. Aeppli, T. G. Perring, C. D. Frost, T. E. Mason, S.-W. Cheong, and Z. Fisk, *Phys. Rev. Lett.* **86**, 5377 (2001).
- ⁴⁶B. Keimer, N. Belk, R. J. Birgeneau, A. Cassanho, C. Y. Chen, M. Greven, M. A. Kastner, A. Aharony, Y. Endoh, R. W. Erwin, and G. Shirane, *Phys. Rev. B* **46**, 14034 (1992).
- ⁴⁷R. J. Birgeneau, M. Greven, M. A. Kastner, Y. S. Lee, B. O. Wells, Y. Endoh, K. Yamada, and G. Shirane, *Phys. Rev. B* **59**, 13788 (1999).
- ⁴⁸L. L. Miller, X. L. Wang, S. X. Wang, C. Stassis, D. C. Johnston, J. Faber, and C.-K. Loong, *Phys. Rev. B* **41**, 1921 (1990).
- ⁴⁹H. S. Choi, Y. S. Lee, T. W. Noh, E. J. Choi, Y. Bang, and Y. J. Kim, *Phys. Rev. B* **60**, 4646 (1999).
- ⁵⁰M. Greven, R. J. Birgeneau, Y. Endoh, M. A. Kastner, M. Matsuda, and G. Shirane, *Z. Phys. B* **96**, 465 (1995).
- ⁵¹D. Vaknin, S. K. Sinha, C. Stassis, L. L. Miller, and D. C. Johnston, *Phys. Rev. B* **41**, 1926 (1990).
- ⁵²M. Al-Mamouri, P. P. Edwards, C. Graeves, and M. Slaski, *Nature (London)* **369**, 382 (1994).
- ⁵³I. de P. R. Moreira, D. Muñoz, F. Illas, C. de Graaf, and M. A. Garcia-Bach, *Chem. Phys. Lett.* **345**, 183 (2001).
- ⁵⁴D. Muñoz, I. de P. R. Moreira, and F. Illas, *Phys. Rev. B* **65**, 224521 (2002).
- ⁵⁵P. R. Slater, P. P. Edwards, C. Greaves, I. Gameson, J. P. Hodges, M. G. Francesconi, M. Al-Mamouri, and M. Slaski, *Physica C* **241**, 151 (1995).
- ⁵⁶D. N. Argyriou, J. D. Jorgensen, R. L. Hitterman, Z. Hiroi, N. Kobayashi, and M. Takano, *Phys. Rev. B* **51**, 8434 (1995).
- ⁵⁷D. Vaknin, L. L. Miller, and J. L. Zarestky, *Phys. Rev. B* **56**, 8351 (1997).
- ⁵⁸D. Hechel and I. Felner, *Physica C* **235-240**, 1601 (1994).
- ⁵⁹Z. Hiroi, N. Kobayashi, and M. Takano, *Physica C* **266**, 191 (1996).
- ⁶⁰D. L. Novikov, A. J. Freeman, and J. D. Jorgensen, *Phys. Rev. B* **51**, 6675 (1995).
- ⁶¹M. Z. Hasan, E. D. Isaacs, Z.-X. Shen, L. L. Miller, K. Tsutsui, T. Tohyama, and S. Maekawa, *Science* **288**, 1811 (2000).
- ⁶²F. Ronning, C. Kim, K. M. Shen, N. P. Armitage, A. Damascelli, D. H. Lu, D. L. Feng, Z.-X. Shen, L. L. Miller, Y.-J. Kim, F. Chou, and I. Terasaki, *Phys. Rev. B* **67**, 035113 (2003).
- ⁶³F. Ronning, T. Sasagawa, Y. Kohsaka, K. M. Shen, A. Damascelli, C. Kim, T. Yoshida, N. P. Armitage, D. H. Lu, D. L. Feng, L. L. Miller, H. Takagi, and Z. X. Shen, *Phys. Rev. B* **67**, 165101 (2003).
- ⁶⁴A. Ino, C. Kim, M. Nakamura, T. Yoshida, T. Mizokawa, Z.-X. Shen, A. Fujimori, T. Kakeshita, H. Eisaki, and S. Uchida, *Phys. Rev. B* **62**, 4137 (2000).
- ⁶⁵R. M. Martin, *Electronic Structure* (Cambridge University Press, Cambridge, U.K., 2004).
- ⁶⁶See, for instance, *Quantum Mechanical Ab-Initio Calculation of the Properties of Crystalline Materials*, Lecture Notes in Chemistry, edited by C. Pisani (Springer-Verlag, Heidelberg, 1992), Vol. 67.
- ⁶⁷R. Dovesi, B. Civalieri, R. Orlando, C. Roetti, and V. R. Saunders, in *Ab Initio Quantum Simulation in Solid State Chemistry Reviews in Computational Chemistry*, edited by K. B. Lipkowitz, R. Larter, and T. R. Cundari (Wiley, New York, 2005),

- Vol. 21, Chap. 1.
- ⁶⁸J. P. Perdew, K. Burke, and M. Ernzerhof, *Phys. Rev. Lett.* **78**, 136 (1997).
- ⁶⁹C. Adamo and V. Barone, *J. Chem. Phys.* **110**, 6158 (1999).
- ⁷⁰M. Ernzerhof and G. E. Scuseria, *J. Chem. Phys.* **110**, 5029 (1999).
- ⁷¹L. A. Curtiss, K. Raghavachari, P. C. Redfern, and J. A. Pople, *J. Chem. Phys.* **106**, 1063 (1997).
- ⁷²P. J. Stephens, F. J. Devlin, C. F. Chabalowski, and M. J. Frisch, *J. Phys. Chem.* **98**, 11623 (1994).
- ⁷³P. E. Blöchl, *Phys. Rev. B* **50**, 17953 (1994).
- ⁷⁴G. Kresse and D. Joubert, *Phys. Rev. B* **59**, 1758 (1999).
- ⁷⁵G. Kresse and J. Hafner, *Phys. Rev. B* **48**, 13115 (1993).
- ⁷⁶G. Kresse and J. Furthmüller, *Comput. Mater. Sci.* **6**, 15 (1996).
- ⁷⁷R. Dovesi, V. R. Saunders, C. Roetti, R. Orlando, C. M. Zicovich-Wilson, F. Pascale, B. Civalieri, K. Doll, N. M. Harrison, I. J. Bush, Ph. D'Arco, and M. Llunell, *CRYSTAL2006 User's Manual* (University of Torino, Torino, 2006).
- ⁷⁸P. J. Hay and W. R. Wadt, *J. Chem. Phys.* **82**, 270 (1985).
- ⁷⁹The standard basis sets can be obtained from the web at <http://www.chimifm.unito.it/> (CRYSTAL site) or <http://www.tcm.phy.cam.ac.uk/~mdt26/crystal.html>
- ⁸⁰P. Rivero, I. de P. R. Moreira, and F. Illas, *J. Phys.: Conf. Ser.* **117**, 012025 (2008).
- ⁸¹D. Muñoz, I. de P. R. Moreira, and F. Illas, *Phys. Rev. Lett.* **84**, 1579 (2000).
- ⁸²A. Kanigel, A. Keren, Y. Eckstein, A. Knizhnik, J. S. Lord, and A. Amato, *Phys. Rev. Lett.* **88**, 137003 (2002).
- ⁸³A. M. Toader, J. P. Goff, M. Roger, N. Shannon, J. R. Stewart, and M. Enderle, *Phys. Rev. Lett.* **94**, 197202 (2005).
- ⁸⁴I. de P. R. Moreira, C. J. Calzado, J. P. Malrieu, and F. Illas, *Phys. Rev. Lett.* **97**, 087003 (2006).
- ⁸⁵I. de P. R. Moreira, C. J. Calzado, J. P. Malrieu, and F. Illas, *New J. Phys.* **9**, 369 (2007).
- ⁸⁶I. de P. R. Moreira, F. Illas, C. J. Calzado, J. F. Sanz, J. P. Malrieu, N. Ben Amor, and V. Maynau, *Phys. Rev. B* **59**, R6593 (1999).
- ⁸⁷Y. J. Kim, J. P. Hill, C. A. Burns, S. Wakimoto, R. J. Birgeneau, D. Casa, T. Gog, and C. T. Venkataraman, *Phys. Rev. Lett.* **89**, 177003 (2002).
- ⁸⁸V. I. Anisimov, F. Aryasetiawan, and A. I. Lichtenstein, *J. Phys.: Condens. Matter* **9**, 767 (1997).
- ⁸⁹F. W. Bader, *Atoms in Molecules: A Quantum Theory* (Oxford Science, Oxford, U. K., 1990).
- ⁹⁰J. Wojdel, I. de P. R. Moreira, and F. Illas, *J. Am. Chem. Soc.* **131**, 906 (2009).
- ⁹¹J. C. Wojdel, I. de P. R. Moreira, S. T. Bromley, and F. Illas, *J. Mater. Chem.* **19**, 2032 (2009).
- ⁹²R. L. Martin and F. Illas, *Phys. Rev. Lett.* **79**, 1539 (1997).